

Supplementary files

The DEAH-box RNA helicase Dhr1 contains a remarkable carboxyl terminal domain essential for small ribosomal subunit biogenesis

Amlan Roychowdhury¹, Clément Joret², Gabrielle Bourgeois¹, Valérie Heurgué-Hamard³,

Denis L.J. Lafontaine^{2,*} and Marc Graille^{1,*}

¹ BIOC, CNRS, Ecole polytechnique, IP Paris, F-91128 Palaiseau, France.

² RNA Molecular Biology, Fonds de la Recherche Scientifique (F.R.S.-FNRS), Université Libre de Bruxelles, Charleroi-Gosselies, Belgium.

³ UMR8261 CNRS-Université de Paris, Institut de Biologie Physico-Chimique, Paris, France.

* Correspondence:

denis.lafontaine@ulb.ac.be; Tel: +32-2-650-9771

marc.graille@polytechnique.edu; Tel.: +33-16-933-4890

Keywords: rRNA maturation, helicase, translation, ribosome synthesis.

Running title: Structure of Dhr1 helicase module

Supplementary Materials and Methods

Over-expression and purification of Dhr1 proteins

The DNA sequence encoding Dhr1 helicase module (amino acids 315 to 1267, hereafter referred to as Dhr1-Hel) was PCR amplified from *S. cerevisiae* genomic DNA using primers oMG208/oMG209 (Table S1). This PCR product was further cloned using *Bgl*II/*Bam*HI and *Xho*I restriction sites into the pGEX-6P-1 expression vector (GE Healthcare Biosciences) to yield pMG718 plasmid encoding for GST-Dhr1-Hel. This fusion protein was expressed at 37°C using *Escherichia coli* BL21 (DE3) Gold cells and 1 L of 2xYT media containing ampicillin (100 µg/mL). Protein expression was induced by adding 500 µM IPTG at OD_{600nm} 0.6 and incubating cells overnight at 20 °C. Cells were harvested, resuspended in buffer A (20 mM Tris-HCl pH 7.5, 200 mM NaCl and 5 mM β-mercaptoethanol) and finally lysed by sonication. After clarification by high speed centrifugation, supernatant was loaded onto Glutathione Sepharose 4B resin (GE Healthcare Biosciences), pre-equilibrated with buffer A. The column was then washed with first 30 mL of buffer A and then 20 mL of buffer W (20 mM Tris-HCl pH 7.5, 2 M NaCl and 5 mM β-mercaptoethanol). Next, the column was washed again with 15 mL of buffer A to decrease NaCl concentration. Recombinant GST-Dhr1-[315-1267] was finally eluted with buffer A supplemented with 25 mM reduced glutathione. After an overnight incubation with human rhinovirus 3C protease at 4°C under dialysis condition against buffer A to remove the glutathione, the sample was loaded on a 5 mL Heparin column (HiTrap Heparin HP from GE Healthcare Biosciences) pre-equilibrated with buffer B (20 mM Tris-HCl pH 7.5, 50 mM NaCl and 5 mM β-mercaptoethanol). Elution was performed by a linear gradient of buffer B/buffer C (20 mM Tris-HCl pH 7.5, 1 M NaCl and 5 mM β-mercaptoethanol) from 100%/0% to 0%/100%. Dhr1 helicase module eluted at approximately 600 mM NaCl. Finally, the protein was purified to homogeneity using a HiLoad 16/60 Superdex 200 column (GE Healthcare Biosciences) pre-equilibrated with buffer D (20 mM Tris-HCl pH 7.5, 150 mM NaCl, 1 mM MgCl₂ and 5 mM β-mercaptoethanol).

The plasmids encoding the Dhr1-[315-1175] (hereafter referred as Dhr1-Hel-ΔCTD; pMG922) and Dhr1-[315-1188] (hereafter referred as Dhr1-Hel-ΔCter; pMG923) fragments were obtained by introducing a stop codon in pMG718 using oligonucleotides oMG481/oMG482 and oMG483/oMG484, respectively. Those fragments were purified as described for Dhr1-Hel fragment.

Over-expression and purification of full-length Utp14

The DNA sequence encoding for full-length Utp14 was PCR amplified from *S. cerevisiae* genomic DNA using primers oMG395/oMG396 (Table S1). This PCR product was further cloned using *Nco*I and *Xho*I restriction sites into the pET28b expression vector to yield pMG817 plasmid encoding for N-terminally His₆-tagged Utp14. The protein was expressed at 37°C using *Escherichia coli* Codon+ cells and 1 L of auto-inducible terrific broth media (ForMedium AIMTB0260) containing kanamycin (100 µg/mL) and chloramphenicol (25 µg/mL). After 3 h growth at 37°C, cells were incubated overnight at 18 °C. Cells were harvested, resuspended in buffer A. Following sonication, cells were incubated with benzonase for 30 minutes at 4 °C. After clarification by high speed centrifugation, supernatant was loaded onto Ni-NTA resin (Qiagen), pre-equilibrated with buffer A. The column was then washed with first 30 mL of buffer A and then 30 ml of buffer A supplemented with 20mM imidazole followed by 20 mL of buffer W (20 mM Tris-HCl pH 7.5, 2 M NaCl and 5 mM β-mercaptoethanol). Next, the column was washed again with 15 mL of buffer A to decrease

NaCl concentration. Recombinant Utp14 was finally eluted with buffer A supplemented with 400mM imidazole. The eluted sample was loaded on a 5 mL Heparin column (HiTrap Heparin HP from GE Healthcare Biosciences) pre-equilibrated with buffer B (20 mM Tris-HCl pH 7.5, 50 mM NaCl and 5 mM β -mercaptoethanol). Elution was performed by a linear gradient of NaCl from 50 mM to 1 M using Buffer C (20 mM Tris-HCl pH 7.5, 1 M NaCl and 5 mM β -mercaptoethanol). Utp14 was eluted at approximately 700 mM NaCl.

Crystallization, data collection and structure determination

Initial very thin plate crystals were obtained by mixing 150 nL of concentrated Dhr1-Hel protein (8 mg/mL in buffer D) with an equal volume of crystallization solution (0.1 M Tris pH 8.5; 8% (w/v) PEG 8000) at 4°C. The initial crystallization conditions were further optimized by hanging drop vapor diffusion method with increased drop volume (2 – 4 μ L) and variable protein concentrations (5 mg/mL to 15 mg/mL) at 4°C. Those crystals suffered from severe anisotropic diffraction and diffraction quality crystals could only be obtained thanks to limited proteolysis. The purified protein (9 mg/mL) was incubated with trypsin (1:500 dilution w/w) for 30 minutes at 20°C prior to crystallization trials using the following crystallization condition: 0.2 M MgCl₂; 0.1 M Tris pH 8.5 and 20% (w/v) PEG 8000. This yielded thicker crystals and single crystals were cryo-protected using mother liquor supplemented with 30% v/v ethylene glycol before flash freezing in liquid nitrogen.

The diffraction data were collected at Proxima-1 beamline (SOLEIL synchrotron, FRANCE) and processed with XDS (1). The crystals diffracted up to 2.3 Å resolution and belonged to space group P2₁2₁2₁ with one molecule in the asymmetric unit. Statistics for data processing are provided in Table S2. The structure of Dhr1 helicase module was solved by molecular replacement method with PHASER program (2) using the coordinates of the isolated domains of *S. cerevisiae* Prp43 as search models (3). Rigid body refinement was performed by REFMAC (4) and successive cycles of restrained refinement and model building were done by BUSTER (5) and COOT (6), respectively, to yield a final structure refined at 2.3 Å resolution with R= 20.5% and R_{free}= 24.5%. The C-terminal domain for which no clear structural model was known, was modeled into the 2Fo-Fc and Fo-Fc electron density maps during the iterative cycles of building and refinement. Due to the absence of electron density map, the following regions were omitted from the final model: 315-372, 647-709, 947-977 and 1054-1058. These regions are either too flexible or have been trimmed by the trypsin treatment needed to obtain diffraction quality crystals. All residues display main-chain dihedral angles that fall within the allowed regions of the Ramachandran plot, as defined by the MOLPROBITY server (7). The final model also contains 276 water molecules, 14 ethylene glycol molecules, one magnesium ion and 4 chlorine ions.

Generation of antibodies directed against full length Dhr1

The DNA sequence encoding for full length Dhr1 was PCR amplified from *S. cerevisiae* genomic DNA (strain BY4741) using primers Dhr1NdeI_989 and Dhr1His6_4840C (Table S1). This PCR product was further cloned using *Bg*II/*Bam*HI and *Nde*I restriction sites into the pET24 expression vector to yield pVH503 plasmid encoding for Dhr1 with a His₆ tag on its C terminus.

Protein over-expression was performed at 37°C using *Escherichia coli* BL21 (DE3) Codon⁺ cells and 1 L of 2xYT media containing kanamycin (50 μ g/mL) and chloramphenicol (25 μ g/mL). Protein expression was

induced by adding 500 μ M IPTG at OD_{600nm} 0.6 and incubating cells overnight at 18°C. Cells were harvested, resuspended in buffer A and finally lysed by sonication. After clarification by high speed centrifugation, supernatant was loaded onto Ni-NTA resin (Qiagen), pre-equilibrated with buffer A. The column was then washed with first buffer A supplemented with 20 mM Imidazole (30 ml) and then 20 mL of buffer W. Finally, the column was washed again with 15 mL of buffer A to remove excess salt. Recombinant Dhr1 FL was finally eluted with buffer A supplemented with 400 mM Imidazole. The eluted protein was further purified first on a 5 mL Heparin column (HiTrap Heparin HP from GE Healthcare Biosciences) and then on a HiLoad 16/60 Superdex 200 Column (GE Healthcare Biosciences) in the same conditions as those described for Dhr1 helicase module.

Anti-Dhr1 antibodies were obtained from Covalab following injection of recombinant full-length *S. cerevisiae* Dhr1 protein into rabbits.

Size Exclusion Chromatography - Multi-Angle Laser Light Scattering (SEC-MALLS)

A 100 μ L sample of Dhr1-Hel (2 mg/mL) was injected at a flow rate of 0.75 mL/min on a Superdex™ 200 10/300 GL column (GE-Healthcare) in buffer A (200 mM NaCl, 20 mM Tris-HCl pH 7.5, 5 mM β -mercaptoethanol). Elution was followed by a UV-Visible spectrophotometer, a RID-20A refractive index detector (Shimadzu), a MiniDawn TREOS detector (Wyatt Technology). The data were collected and processed with the program ASTRA 6.1 (Wyatt Technology). M_w was directly calculated from the absolute light scattering measurements using a dn/dc value of 0.183.

ATPase assay

GST-Dhr1-Hel WT, GST-Dhr1-Hel K420A mutant, GST-Dhr1-Hel- Δ Cter, GST-Dhr1-Hel- Δ CTD and GST (negative control) were assayed for their RNA-dependent ATPase activity by the malachite green method. Each reaction mixture (200 μ L) contained 50 mM Tris-HCl pH 8.0, 40 mM KCl, 1 mM MgCl₂, 15 mM NaCl, 2 mM sodium acetate, 2 mM DTT, 4 mg/mL poly(A) (Sigma; #P9403), 4% (v/v) glycerol and 0.5 μ M enzyme. Reactions were performed in 96 well microplates. The reaction was initiated by rapid addition of ATP (final concentration 1 mM) and quenched after 1 minute by addition of 7 μ L of 0.5 M EDTA. For phosphate dosage, 150 μ L of Malachite green reagent was added to each well and OD_{620nm} read rapidly using Multiskan Spectram from Thermo labsystems. The quantity of phosphate released in 1 min for each reaction was determined by the phosphate standard curve. Each set of experiment was performed in triplicates.

Yeast strains and plasmids

Yeast cells were cultured at 30°C in synthetic minimal medium: 2% glucose (Sigma, #G7021), yeast nitrogen base (Formedium, #CYN0505), supplemented with the required amino acids, according to standard procedures.

To produce yeast strains expressing C-terminally truncated versions of DHR1, diploid cells (BY4743, available from Euroscarf) were transformed with suitable PCR cassettes produced using oligonucleotides LD4221 and LD4222 (for Dhr1 Δ Cter) or LD4220 and LD4221 (for Dhr1 Δ CTD; see Table S1 for details) and plasmid pDL787. Clones selected on minimum medium lacking uracil were diagnosed by PCR on genomic DNA and by DNA sequencing of the junctions using primers LD2794 and LD268 (Table S1).

For conditional expression of Dhr1 mutants, an haploid yeast strain expressing DHR1 under the control of a regulatable pMET promoter (pMET::HA-dhr1; (8)) was transformed with a low-copy plasmid expressing wild-type DHR1 under its own promoter and terminator sequences (pDL0964), or a derivative of this construct carrying a carboxyl terminal truncation (Dhr1 Δ Cter in pDL1031; Dhr1 Δ CTD in pDL1010), or a point mutation (K420A in plasmid pDL0976, N570K in pDL0977, K637H in pDL0978, or L639P in pDL0979), or the empty control plasmid (pFL36; (9)). Plasmid pDL0964 was produced by homologous recombination in yeast by inserting a genomic fragment of DHR1 isolated by *Pvu*II/*Eco*RV digestion from plasmid pTL93 into pFL36 (ARS/CEN-LEU2) cleaved by *Bam*HI/*Hind*III. To produce pTL93, a genomic fragment of DHR1 was isolated from pTL92 by *Xba*I/*Sph*I digestion and cloned into pFL44S (2 μ m-URA3) digested by *Sal*II/*Sph*I digestion. To produce pTL92, a genomic fragment encoding DHR1 was retrieved from the ATCC plasmid Ref #70976 by *Pst*I/*Eco*RV digestion and cloned into pUC18 digested by *Sma*I/*Pst*I. Point mutations were introduced into pDL0964 directly by site-directed mutagenesis using a site directed mutagenesis kit (Quick change, Agilent, #200523). The plasmids were diagnosed by restriction digests and DNA sequencing using oligonucleotides LD803-805, LD1136, LD1150 and LD2643. For site-directed mutagenesis of DHR1, the oligonucleotides (Table S1) used were oMG367 and oMG368 (to produce the K420A mutation); oMG475 and oMG476 (for N570K mutation); oMG477 and oMG478 (for K637H); and oMG479 and oMG480 (for L639P). Plasmids pDL1010 and pDL1031 were produced by homologous recombination in yeast by co-transformation of a synthetic gene fragment (gBlocks, IDT: gDL0020 for pDL1010, and gDL0022 for pDL1031) into pDL0964 cleaved by *Bpu*I/*Sma*I. pDL1010 and pDL1031 were diagnosed by restriction digests and DNA sequencing using oligonucleotides LD803-LD805 and LD4326.

Supplementary figure legends

Figure S1: Structural comparison of Dhr1-Hel and Prp43 from *S. cerevisiae*

For the sake of clarity, the secondary structure elements (α helices and β sheets) are only labelled for Dhr1 in all three panels.

- A. Superimposition of RecA1 domains ('right fingers') from Dhr1 (light green; this work) and Prp43 (grey; (10)). The rmsd value calculated between these two domains is 1.36 \AA over 177 C α atoms (48% sequence identity).
- B. Superimposition of RecA2 domains ('left fingers') from Dhr1 (dark green; this work) and Prp43 (grey; (10)). The rmsd value calculated between these two domains is 1.1 \AA over 164 C α atoms (43% sequence identity).
- C. Superimposition of Dhr1 (with WH, HB, and OB-fold color-coded in purple, salmon, and cyan, respectively) and Prp43 (grey) auxiliary modules. The rmsd value calculated between these two domains is 1.83 \AA over 243 C α atoms (26% sequence identity). To generate this figure, the structure of Prp43 bound to RNA and ADPNP (10) has been used but the same result (1.93 \AA over 243 C α atoms) is obtained for Prp43 bound to ADP (3).

Figure S2: Sequence alignment of Dhr1 and Prp43 RecA1 and RecA2 domains

Strictly conserved residues are in white on a black background. Partially conserved residues are boxed. Secondary structure elements observed in *S. cerevisiae* Dhr1-Hel crystal structure are indicated above the alignment. Residues involved in ADPNP binding in *S. cerevisiae* Prp43 structure are indicated by black stars. DEAH helicase motifs are boxed and labeled in red. Sc, *S. cerevisiae*; Kl, *K. lactis*; Dh, *D. hansenii*; Yl, *Y. lypolitica*; Sp, *S. pombe*; Ct, *C. thermophilum*; Ce, *Caenorhabditis elegans*; Dm, *Drosophila melanogaster*; Dr, *Dario rerio*; Hs, *Homo sapiens*. The figure was generated with the ESPript server (11).

Figure S3: Dhr1 harbors a unique carboxyl terminal domain (CTD)

A-B. The 2Fo-Fc (panel A; contoured at 1 σ ; blue) and Fo-Fc (panel B contoured at 3 σ ; green) electron density maps displayed on the ribbon representation of the final CTD model. These maps have been calculated by refining the Dhr1 structure lacking the CTD against the native dataset.

C. The crystallized Dhr1 helicase module is monomeric in solution. A zoom centered on the main peak with the refractive index colored in blue (left y-axis) and the distribution of molecular mass calculated from light scattering along this peak colored in red (right y-axis) is shown. The measured

molecular weight (101.5 kDa) is close from the theoretical one (108.5 kDa) calculated from the protein sequence.

Figure S4: Sequence alignment of Dhr1 auxiliary and C-terminal domains

Strictly conserved residues are in white on a black background. Partially conserved residues are boxed. Secondary structure elements observed in *S. cerevisiae* Dhr1 crystal structure are indicated above the alignment. Residues corresponding to helix α 24 are in a wine red box. Sc, *S. cerevisiae*; Kl, *K. lactis*; Dh, *D. hansenii*; Yl, *Y. lypolitica*; Sp, *S. pombe*; Ct, *C. thermophilum*; Ce, *Caenorhabditis elegans*; Dm, *Drosophila melanogaster*; Dr, *Dario rerio*; Hs, *Homo sapiens*. The figure was produced with the ESPript server (11).

Figure S5: Analysis of doubling time of yeasts expressing single point Dhr1 mutants or truncation of the CTD

Growth was monitored by OD₆₀₀, and doubling time calculated using a tool available at <http://www.doubling-time.com/compute.php>.

Figure S6: The 3' end of single stranded nucleic acids ‘wraps around’ the 3' clamp from RecA1 domain

Zoom on the RecA1 3' clamp region from *S. cerevisiae* Prp43 (grey, A; (10)) or archaeal Hel308 (yellow, B; (12)) bound to a long single stranded nucleic acid (red).

Figure S7: Comparison of open and closed forms of the Dhr1 helicase

The figure shows that in our structure (panel A) the helicase module is ‘open’, with the RNA channel clearly visible and accessible.

A. Surface representation of *S. cerevisiae* Dhr1-Hel in its open/apo form. The same color code as in Figure 2 is used. The RNA fragment and nucleotide have been modeled by superimposing the structure of *CtPrp43-RNA-ATP* onto Dhr1-Hel structure and are colored black and magenta, respectively.

B. Surface representation of a model of *S. cerevisiae* Dhr1-Hel bound to RNA and ATP. This figure was generated by superimposing the various Dhr1 domains onto the corresponding domains in the structure of *CtPrp43-RNA-ATP*.

C. Surface representation of *CtPrp22* (chain A; (13)) apo-form with the RNA and ATP molecules modeled as in panels A and B shown for the sake of comparison.

D. Surface representation of *CtPrp22* (chain B; (13)) apo-form with the RNA and ATP molecules modeled as in panels A and B shown for the sake of comparison.

Figure S8: The aberrant RNA that accumulates in Dhr1 mutants is 22S

A. High molecular weight RNAs extracted from the indicated strains (see Figure 4 for details) were analyzed by agarose denaturing gel electrophoresis followed by northern blotting with probe LD340 and LD471.

B. Schematics reprinting the structure of yeast pre-rRNA intermediates and northern-blot probes (LD340 and LD471) used. Aberrant RNAs (21S and 22S) are highlighted in red. The 22S extends from sites A0 to A3, resulting from inhibition of cleavage at sites A1/A2, is detected with oligonucleotides LD340 and LD471. The 21S (not detected in Dhr1 mutants and indicated here for reference) extends between sites A1 and A3.

References

1. Kabsch, W. (1993) Automatic processing of rotation diffraction data from crystals of initially unknown symmetry and cell constants. *J. Appl. Cryst.*, **26**, 795-800.
2. McCoy, A.J., Grosse-Kunstleve, R.W., Adams, P.D., Winn, M.D., Storoni, L.C. and Read, R.J. (2007) Phaser crystallographic software. *Journal of Applied Crystallography*, **40**, 658-674.
3. Walbott, H., Mouffok, S., Capeyrou, R., Lebaron, S., Humbert, O., van Tilburgh, H., Henry, Y. and Leulliot, N. (2010) Prp43p contains a processive helicase structural architecture with a specific regulatory domain. *The EMBO journal*, **29**, 2194-2204.
4. Murshudov, G.N., Vagin, A.A. and Dodson, E.J. (1997) Refinement of Macromolecular Structures by the Maximum-Likelihood Method. *Acta Crystallogr D Biol Crystallogr*, **53**, 240-255.
5. Bricogne, G., Blanc, E., Brandl, M., Flensburg, C., Keller, P., Paciorek, W., Roversi, P., Sharff, A., Smart, O.S., Vonrhein, C. *et al.* (2016), Cambridge, United Kingdom: Global Phasing Ltd.
6. Emsley, P., Lohkamp, B., Scott, W.G. and Cowtan, K. (2010) Features and development of Coot. *Acta Crystallogr D Biol Crystallogr*, **66**, 486-501.
7. Davis, I.W., Leaver-Fay, A., Chen, V.B., Block, J.N., Kapral, G.J., Wang, X., Murray, L.W., Arendall, W.B., 3rd, Snoeyink, J., Richardson, J.S. *et al.* (2007) MolProbity: all-atom contacts and structure validation for proteins and nucleic acids. *Nucleic acids research*, **35**, W375-383.
8. Colley, A., Beggs, J.D., Tollervey, D. and Lafontaine, D.L. (2000) Dhr1p, a putative DEAH-box RNA helicase, is associated with the box C+D snoRNP U3. *Molecular and cellular biology*, **20**, 7238-7246.
9. Bonneaud, N., Ozier-Kalogeropoulos, O., Li, G.Y., Labouesse, M., Minvielle-Sebastia, L. and Lacroute, F. (1991) A family of low and high copy replicative, integrative and single-stranded *S. cerevisiae/E. coli* shuttle vectors. *Yeast*, **7**, 609-615.
10. He, Y., Staley, J.P., Andersen, G.R. and Nielsen, K.H. (2017) Structure of the DEAH/RHA ATPase Prp43p bound to RNA implicates a pair of hairpins and motif Va in translocation along RNA. *Rna*, **23**, 1110-1124.

11. Robert, X. and Gouet, P. (2014) Deciphering key features in protein structures with the new ENDscript server. *Nucleic acids research*, **42**, W320-324.
12. Buttner, K., Nehring, S. and Hopfner, K.P. (2007) Structural basis for DNA duplex separation by a superfamily-2 helicase. *Nature structural & molecular biology*, **14**, 647-652.
13. Hamann, F., Enders, M. and Ficner, R. (2019) Structural basis for RNA translocation by DEAH-box ATPases. *Nucleic acids research*.

Table S1: Oligonucleotides

Proteins or mutant	Names	Sequence	Plasmid generated	Purpose
Dhr1-Hel (residues 315 to 1267)	oMG208	GGGAGATCTATGAACGAATTCAAGGATTGG	pMG718 (pGEX6p-1; Amp ^R)	Cloning
	oMG209	CCCCTCGAGTTATTTTTCTTCTCTT-CACC		
Dhr1 (residues 1 to 1267)	Dhr1NdeI_989	AGAAATATACATATGGGTACTTACA-GAAAAAGGTTAACGAAAAGCCA-GATCCGGCCACATGGC	pVH503 (pET24; Kan ^R)	Cloning
	Dhr1-His6_4840C	TTCTATAAGATCTGCGCAT-TAGTGGTGGTGGTGGTGGTTTTCTTCTT-CACCTGTGATGGTCTGG		
Dhr1-Hel-ΔCTD (residues 315 to 1175)	oMG481	CATCGCAAGCTAACCCCTAGCGAACATAGC AAGAAAGG	pMG922 (pGEX6p-1; Amp ^R)	Site directed mutagenesis
	oMG482	CGCTAAGGGTTAGCTTGCATGTCACATAA AGTATTG		
Dhr1-Hel-ΔCter (residues 315 to 1188)	oMG483	CTTCTTTGTAATACAGTAAACCTCTGACTG GTCAAGGC	pMG923 (pGEX6p-1; Amp ^R)	Site directed mutagenesis
	oMG484	GGTTTACTGTATTACAAAAGAAGTCCCTTC TTGCTATG		
Utp14-FL	oMG395	AGCGACCATGGGCCACCACCATCATCACCA TGCAAAAAAGAACATCTAAG	pMG817 (pET28b; Kan ^R)	Cloning
	oMG396	CCAGACTCGAGTTACTTAAATGGTGCCTTC AAAG		
Dhr1-ΔCter and Dhr1-ΔCTD	LD4221	GTTCTTATATAATGAAACTCTATTCTATAAT ACCAGCGCTACGACTCACTATAGGG		Cloning
Dhr1-ΔCter	LD4222	GCACCCCCCTAGCGAACATAGCAAGAAAG GGTCTTCTTGAGCACCACCATCACCACAC C		Cloning
Dhr1-ΔCTD	LD4220	GGAAATAATAAACAAAGGATGAATACTTTAT GTGACATCGCAAGC		Cloning
K420A mutant	oMG367	GGTCAGGTGCGACTACACAAGTCCA- CAATTTTATATG	pDL0976	Site directed mutagenesis
	oMG368	TGTGTAGTCGCACCTGACCCGTTCAC- CACAAATAATC		
N570K mutant	oMG475	TCAGCGAAAAGAAAACATTGTTCCCCA- TAGCGCCCC	pDL0977	Site directed mutagenesis
	oMG476	AATGTTTCTTTCGCTGAAATCTGATACCCCTTAATG		
K637H mutant	oMG477	CACATGGTACACAGGCTAACGAAAG- GAATTCCCTTTAAG	pDL0978	Site directed mutagenesis
	oMG478	CTTAGCCTGTTGACCATGTGTG- TAATTCCTGCTGACCG		
L639P mutant	oMG479	GTAAAAAGGCCTAGAAAGGAATTCCCTT- TAAGAAAAAC	pDL0979	Site directed mutagenesis
	oMG480	TCCTTCTAGGCCTTTTACCATGTGTG- TAATTCCTG		
	LD2794	ATATTCCCTGTTGGCCACG		Sequencing

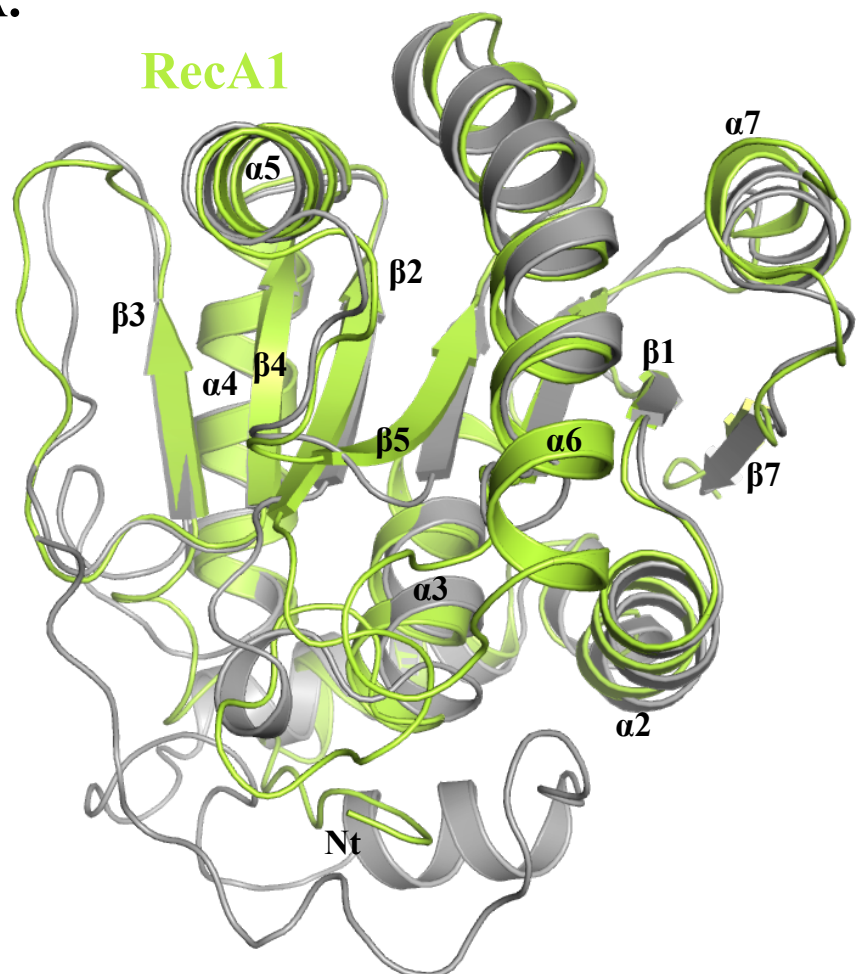
	LD268	GAATTGTTGCCACGGC		Sequencing
	LD803	CCAAAAGTTGGATGAGTATGG		Sequencing
	LD804	GGTAAGACTACACAAGTCCC		Sequencing
	LD805	GGAATTTCCTTTAAGAAAAACTCC		Sequencing
	LD1136	CCTCCAGATAGAGTTGCC		Sequencing
	LD1150	GGTTTGTCGACCATGTTGCCG		Sequencing
	LD2643	GGCTCCTATTTCTAGTTGC		Sequencing
	LD4326	GCGAATCCGGACATCTACTGC		Sequencing
	LD471	CGGTTTAATTGTCC		Northern blot
	LD366	CCAAGTTGGATTCACTGGCTC		Northern blot
	LD340	CCAGATAACTATCTAAAG		Northern blot
Dhr1-ΔCter	gDL0022	5'- AGATGAAGCACATGAAAGAACATTAA CACTG TATTTGATCGGTATGC...[on chromosome XIII DHR1 DNA sequence from 525289 bp to 527978 bp deleted from 527259 bp to 527496 bp]... GGGTACCGAGCTCGAATTCACTGGCCGT CGTTTACACGTCGTGACTGG-3'	pDL1031	Plasmid pro- duction
Dhr1-ΔCTD	gDL0020	5'- AGATGAAGCACATGAAAGAACATTAA CACTG TATTTGATCGGTATGC...[on chromosome XIII DHR1 DNA sequence from 525289 bp to 527978 bp deleted from 527220 bp to 527496 bp]... GGGTACCGAGCTCGAATTCACTGGCCGT CGTTTACACGTCGTGACTGG-3'	pDL1010	Plasmid pro- duction

Table S2: Data collection, phasing and refinement statistics

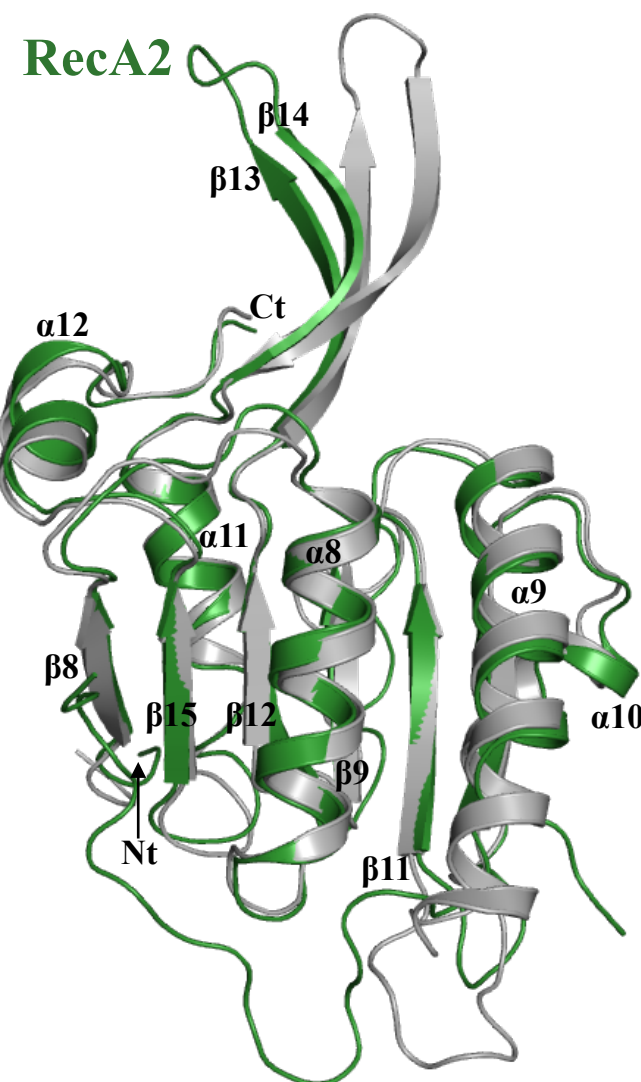
Data collection	
Space group	P2 ₁ 2 ₁ 2 ₁
Unit cell parameters	
<i>a</i> ; <i>b</i> ; <i>c</i> (Å)	57.3; 115.8; 157.5
α ; β ; γ (°)	90; 90; 90
Resolution (Å)	50.0 - 2.3 (2.38-2.30)
R _{meas} (%)	12.8 (112.7)
<i>I</i> / σI	8.6 (1.2)
Completeness (%)	97.1 (98.6)
CC _{1/2} (%)	99.5 (47.6)
Redundancy	3.4
Observed reflections	157599
Unique reflections	45887
Refinement	
Resolution (Å)	48.83 – 2.3
No. reflections	45851
R / R _{free} (%)	20.5/24.5
<i>No. atoms</i>	
Protein	6363
Ligands (Ethylene glycol / ions)	61
Water	276
<i>B</i> -factors (Å ²)	
Protein	45.5
Ethylene glycol / ions	53.3
Water	41.5
<i>R.m.s deviations</i>	
Bond lengths (Å)	0.01
Bond angles (°)	1.15
<i>Ramachandran plot</i>	
Favored regions	97.8 %
Allowed regions	2.2 %

Figure S1

A.



B.



C.

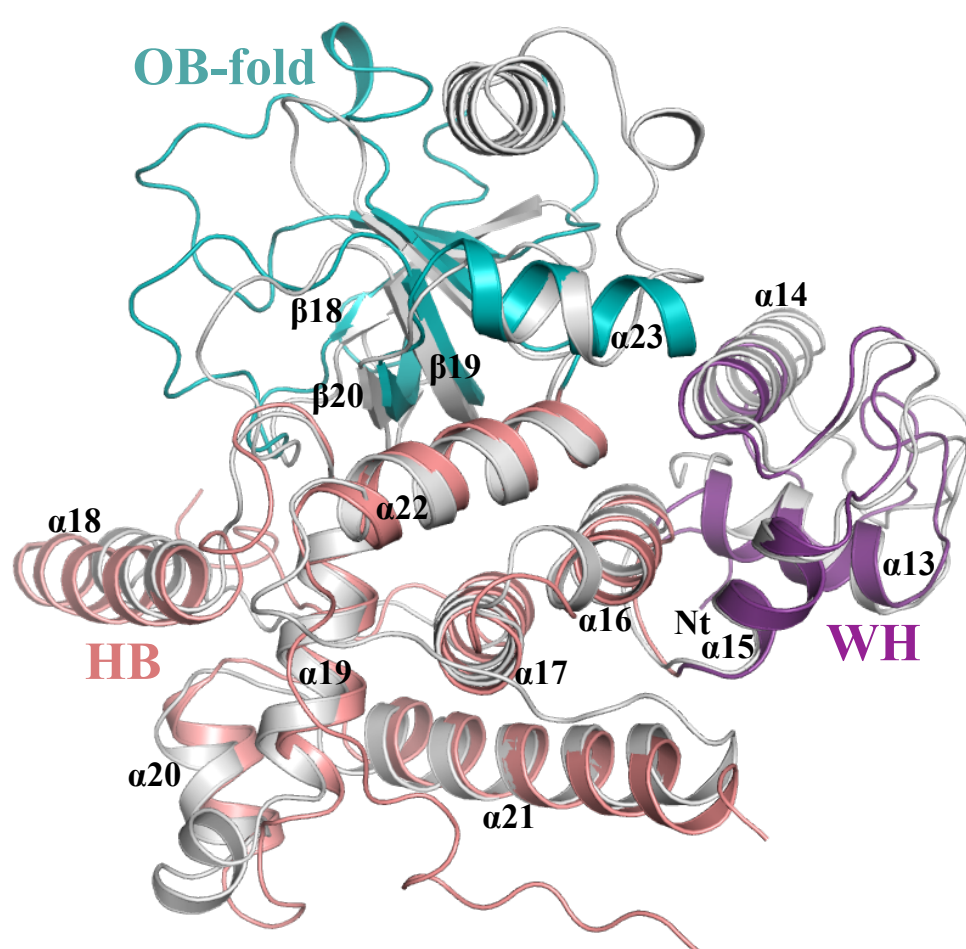


Figure S2

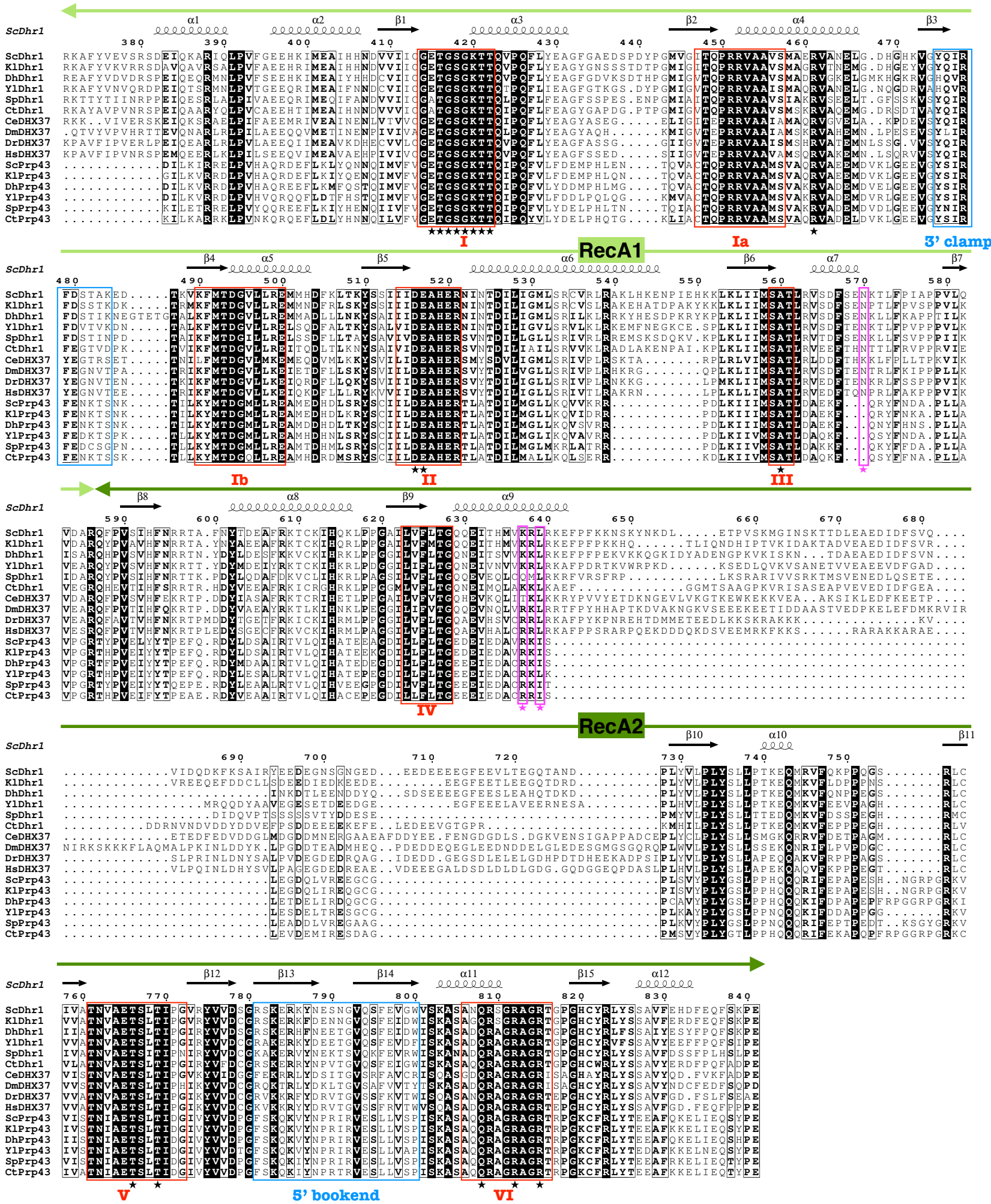


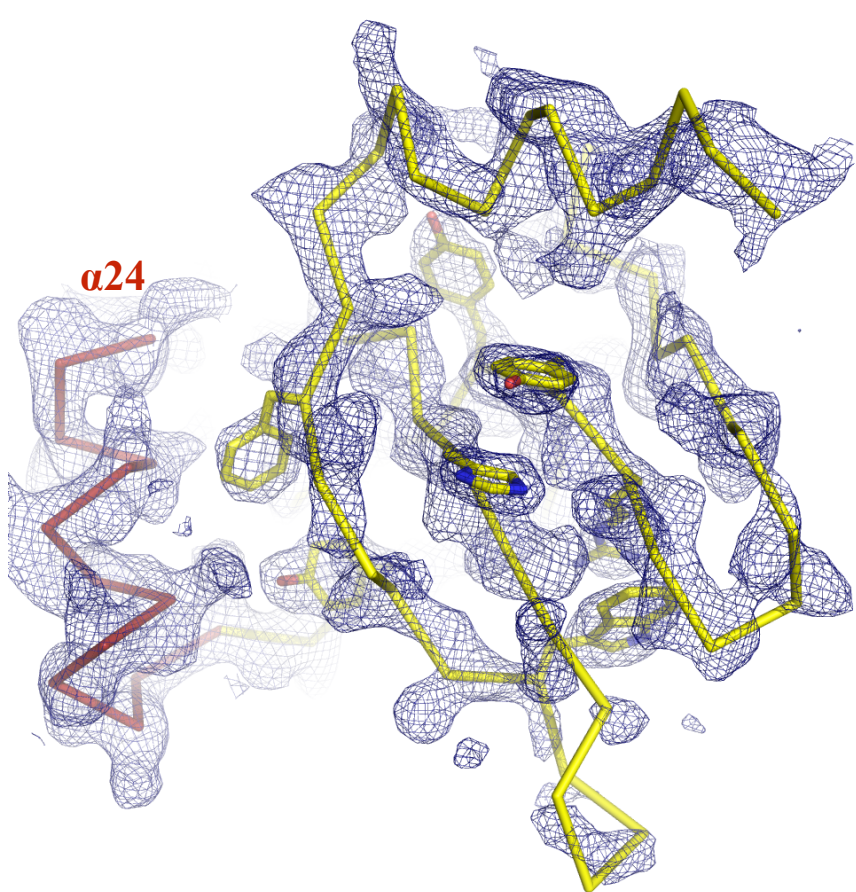
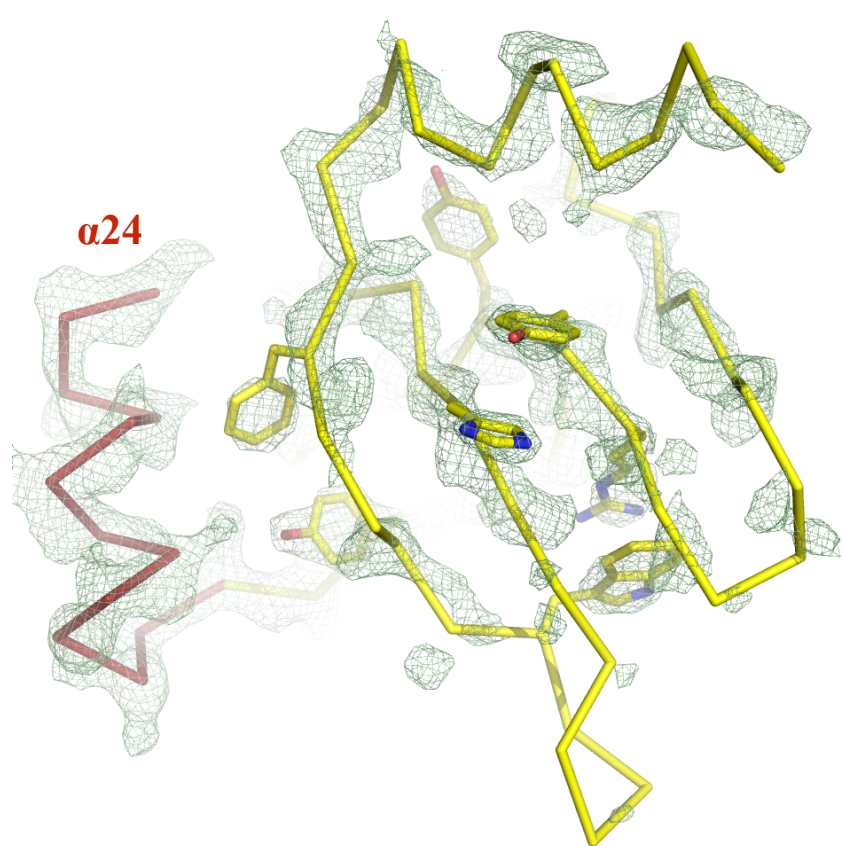
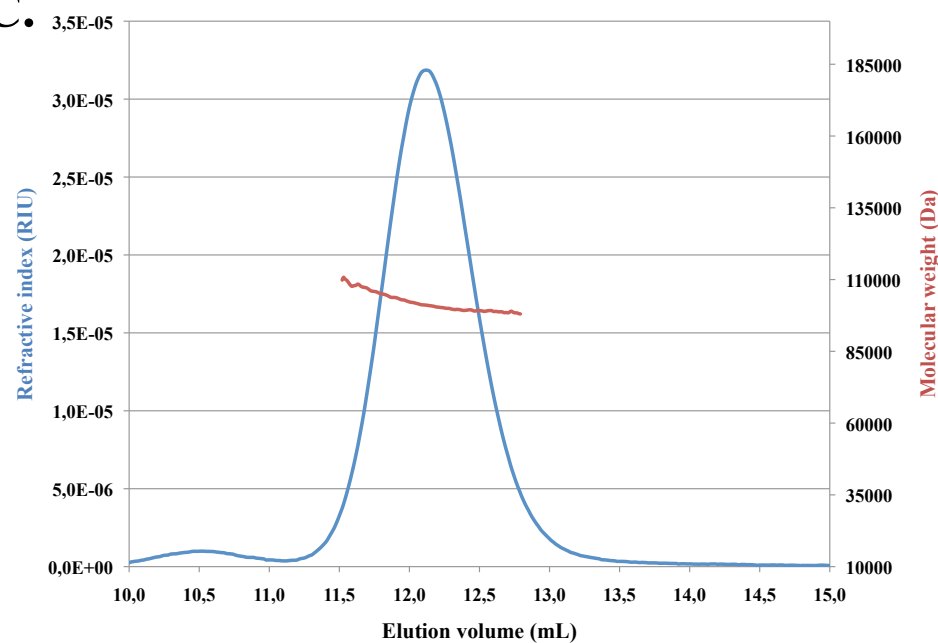
Figure S3**A.****B.****C.**

Figure S4

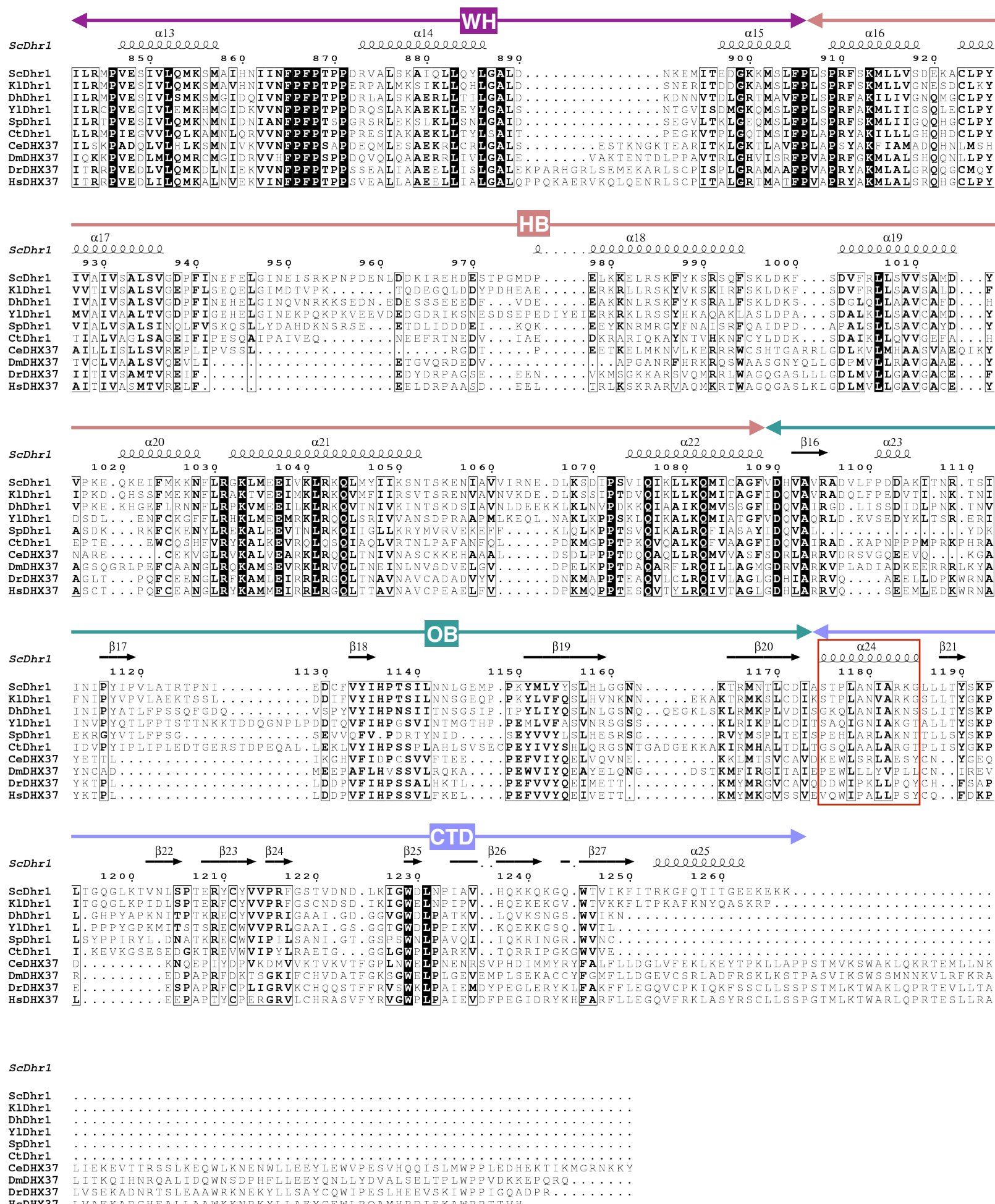
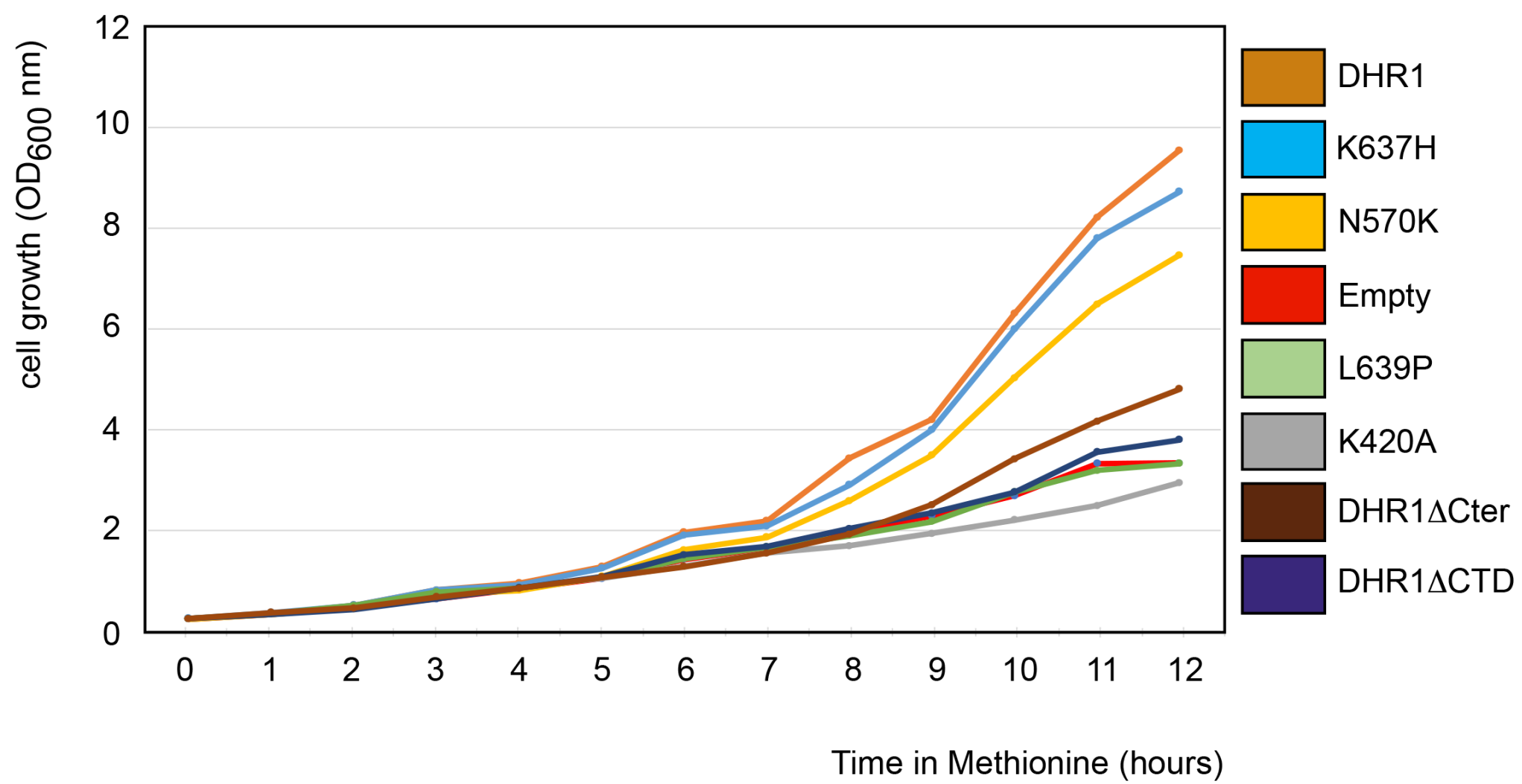
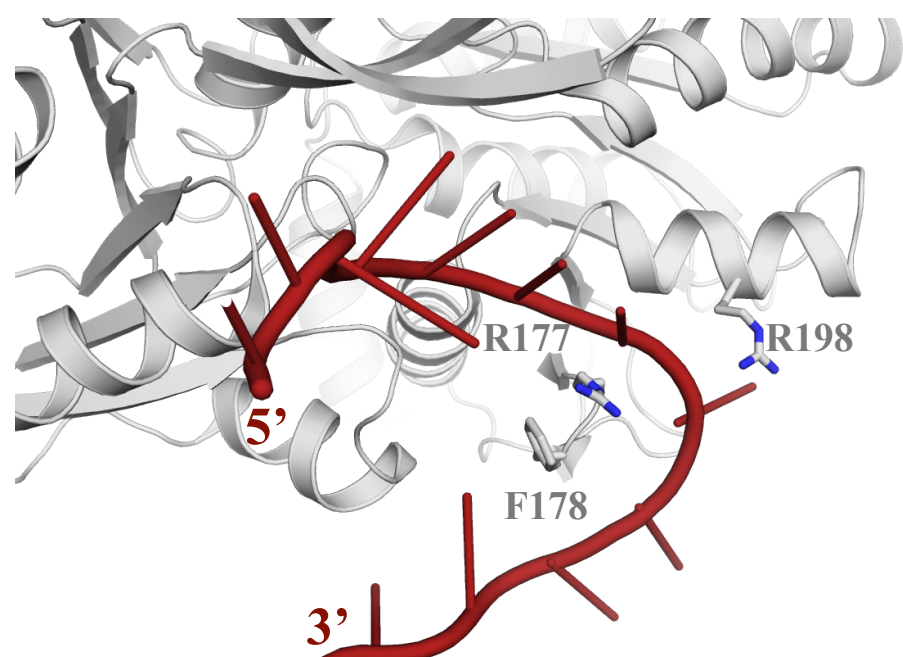


Figure S5

	Empty	DHR1	K420A	N570K	K637H	L639P	DHR1 Δ Cter	DHR1 Δ CTD
DT (hours)	3.15	2.28	3.37	2.44	2.36	3.21	2.97	3.05
% of WT DT	72.3%	100%	67.65%	93.44%	96.61%	73.18%	76.76%	74.75%

Figure S6

A.



B.

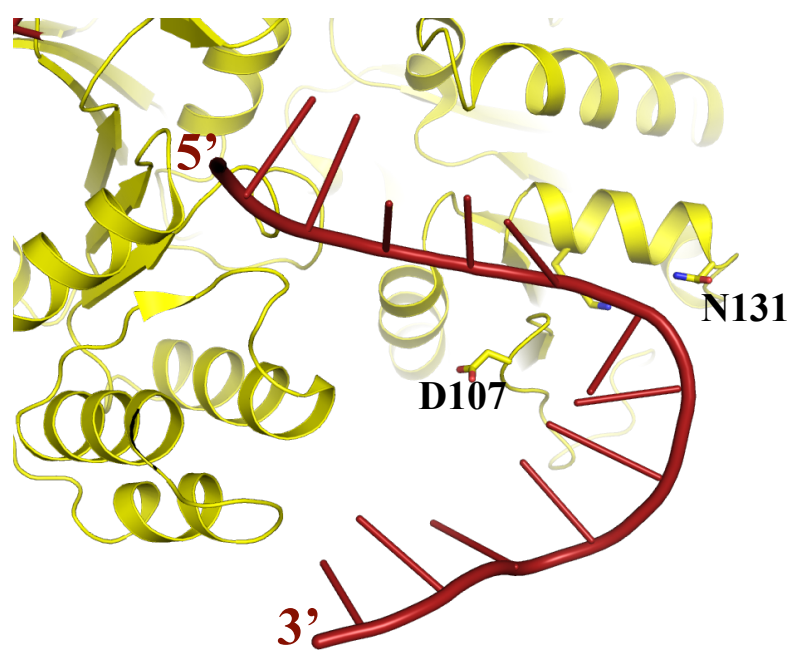
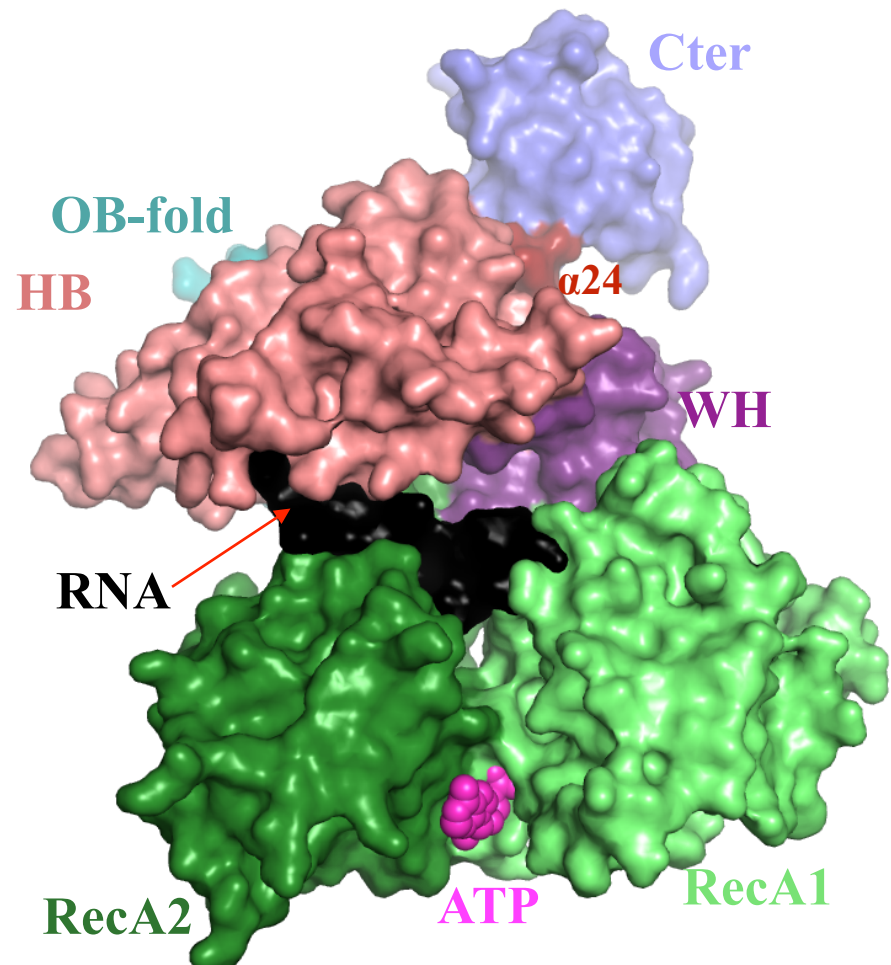
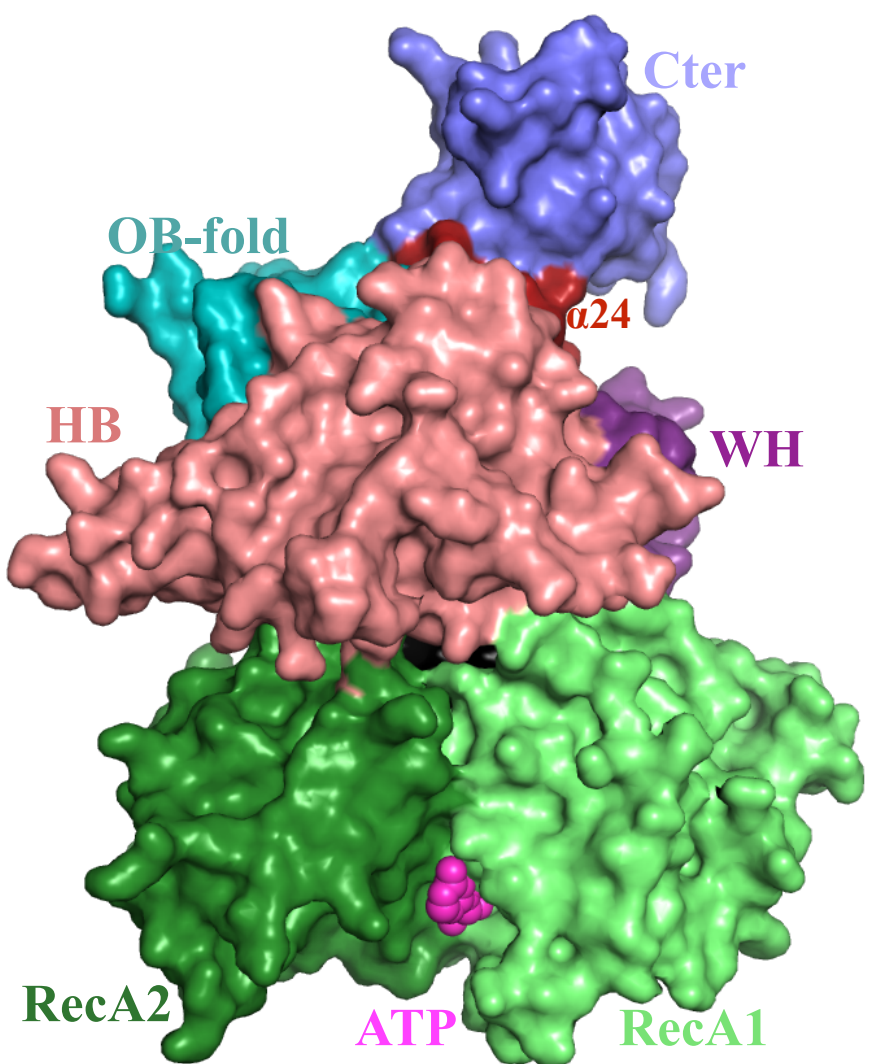


Figure S7

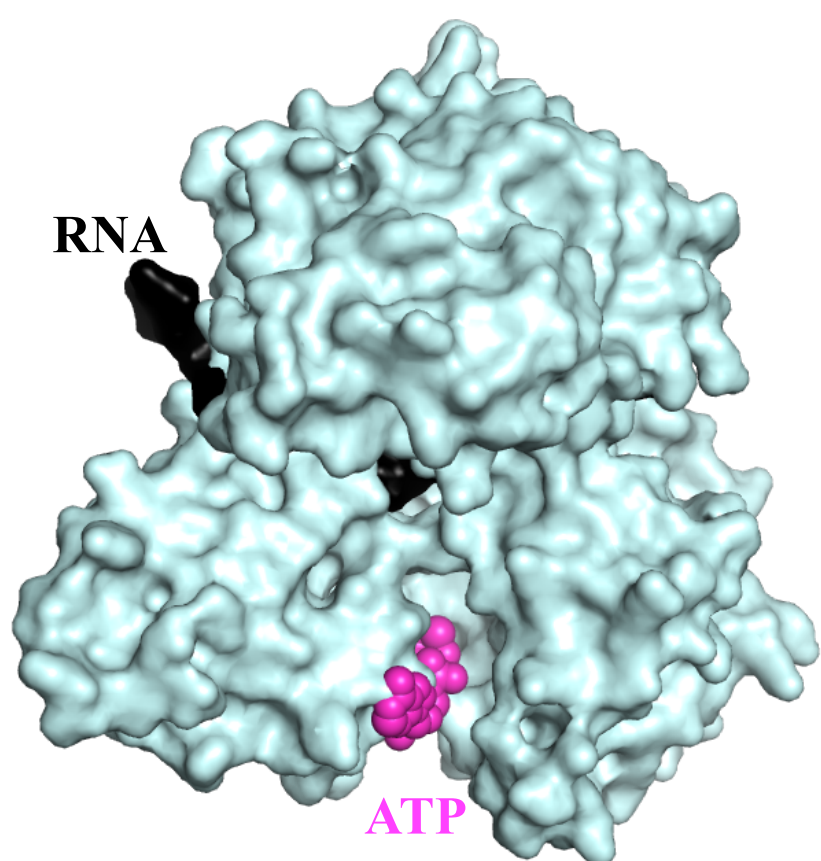
A.



B.



C.



D.

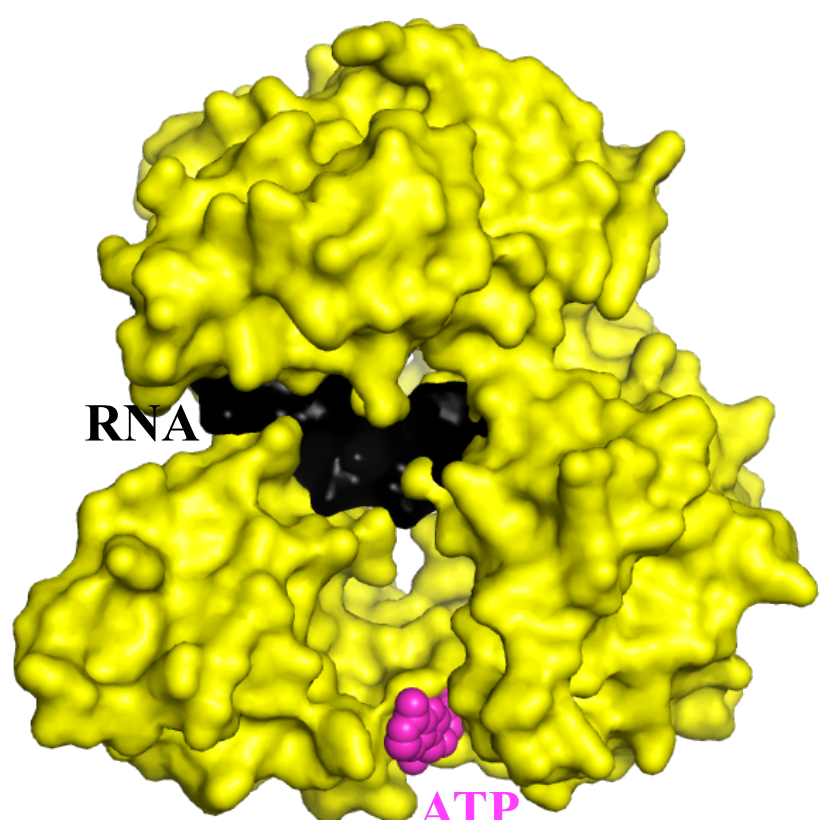
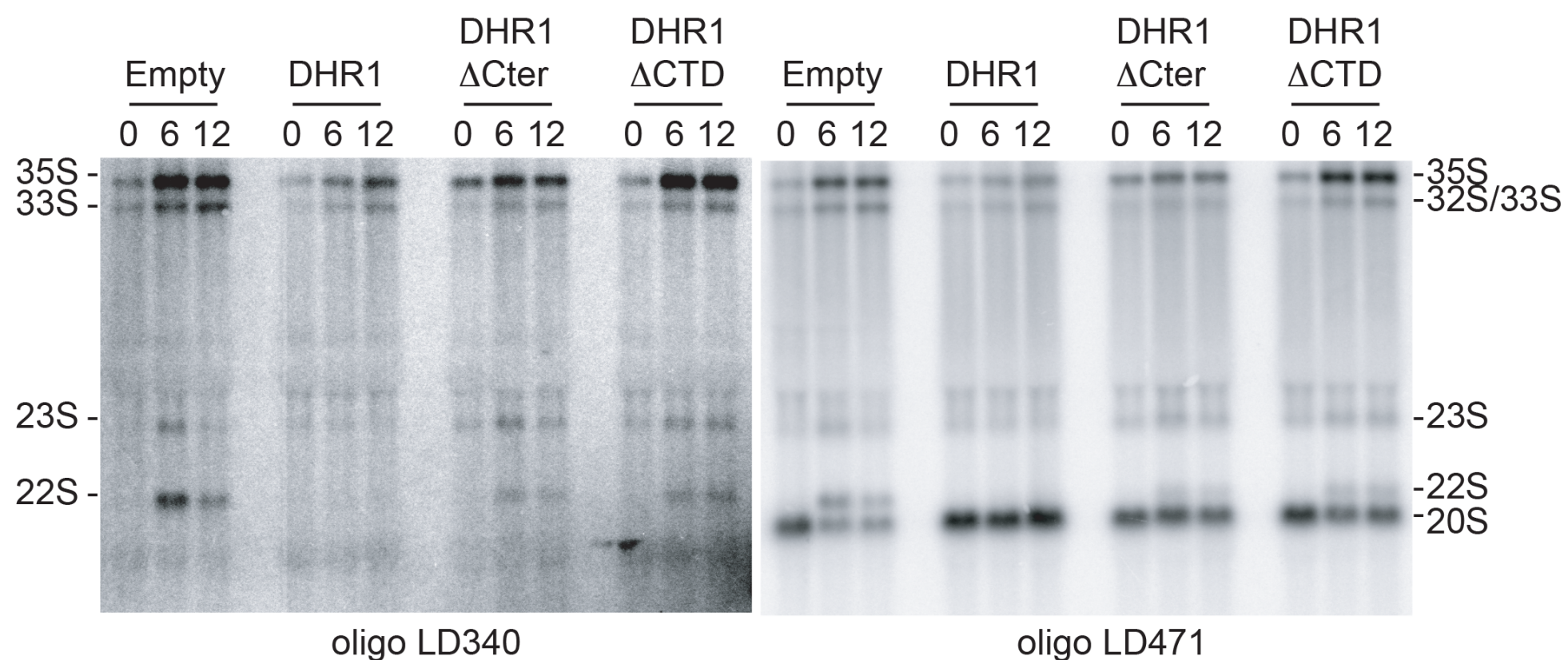


Figure S8

A.



B.

